

Featuring work from the group of Professor R. Bashir in the Department of Bioengineering, Department of Electrical and Computer Engineering, and the Micro and Nanotechnology Laboratory at the University of Illinois, Urbana-Champaign, Urbana, IL USA.

**Title: Multi-material bio-fabrication of hydrogel cantilevers and actuators with stereolithography**

Fabricating biohybrid cantilevers and actuators with hydrogels and cardiac cells using a 3D stereolithographic printer. The multi-material capability of the printer can be used to change the synthetic material composition or insert cells and proteins at precise locations on the structure. Image courtesy of Janet Sinn-Hanlon at the Beckman Institute, University of Illinois, Urbana-Champaign.

As featured in:



See Sabaté *et al.*,  
*Lab Chip*, 2012, **12**, 74.

Cite this: *Lab Chip*, 2012, **12**, 88

www.rsc.org/loc

PAPER

## Multi-material bio-fabrication of hydrogel cantilevers and actuators with stereolithography†

Vincent Chan,<sup>ae</sup> Jae Hyun Jeong,<sup>b</sup> Piyush Bajaj,<sup>ae</sup> Mitchell Collens,<sup>ae</sup> Taher Saif,<sup>d</sup> Hyunjoon Kong<sup>b</sup> and Rashid Bashir<sup>\*ace</sup>

Received 26th July 2011, Accepted 21st October 2011

DOI: 10.1039/c1lc20688e

Cell-based biohybrid actuators are integrated systems that use biological components including proteins and cells to power material components by converting chemical energy to mechanical energy. The latest progress in cell-based biohybrid actuators has been limited to rigid materials, such as silicon and PDMS, ranging in elastic moduli on the order of mega ( $10^6$ ) to giga ( $10^9$ ) Pascals. Recent reports in the literature have established a correlation between substrate rigidity and its influence on the contractile behavior of cardiomyocytes (A. J. Engler, C. Carag-Krieger, C. P. Johnson, M. Raab, H. Y. Tang and D. W. Speicher, *et al.*, *J. Cell Sci.*, 2008, **121**(Pt 22), 3794–3802, P. Bajaj, X. Tang, T. A. Saif and R. Bashir, *J. Biomed. Mater. Res., Part A*, 2010, **95**(4), 1261–1269). This study explores the fabrication of a more compliant cantilever, similar to that of the native myocardium, with elasticity on the order of kilo ( $10^3$ ) Pascals. 3D stereolithographic technology, a layer-by-layer UV polymerizable rapid prototyping system, was used to rapidly fabricate multi-material cantilevers composed of poly (ethylene glycol) diacrylate (PEGDA) and acrylic-PEG-collagen (PC) mixtures. The incorporation of acrylic-PEG-collagen into PEGDA-based materials enhanced cell adhesion, spreading, and organization without altering the ability to vary the elastic modulus through the molecular weight of PEGDA. Cardiomyocytes derived from neonatal rats were seeded on the cantilevers, and the resulting stresses and contractile forces were calculated using finite element simulations validated with classical beam equations. These cantilevers can be used as a mechanical sensor to measure the contractile forces of cardiomyocyte cell sheets, and as an early prototype for the design of optimal cell-based biohybrid actuators.

### Introduction

Cell-based biohybrid actuators are integrated systems that employ elements of biology to power synthetic structures. The biological and synthetic components have a dependent relationship, which pass information in one or both directions; this direct interaction forms a ‘biohybrid’ system. For example, cells are able to sense the mechanical properties of the substrate they

are grown on and respond through biological functions such as migration, differentiation, or proliferation.<sup>3</sup> Driven by cells, biohybrid actuators can be autonomous, or controlled chemically or electrically. Using glucose as a chemical energy source, cells can generate power by converting it to mechanical energy. These systems could be used to promote the design of more effective and intelligent bio-machines (*i.e.* bio-bots<sup>4–6</sup> and power generators<sup>7</sup>), help us understand the emergent behavior of cellular systems, and have applications in drug discovery.

Significant progress in developing cell-based biohybrid actuators has recently been reported. Contractile stresses and forces of single cells and cell sheets of cardiomyocytes and skeletal myotubes cultured on silicon<sup>8</sup> and PDMS<sup>9</sup> micro-cantilevers have been measured. Xi *et al.*<sup>4</sup> developed a microdevice using a silicon backbone with self-assembled cardiomyocytes grown on a chromium/gold layer. The collective and cooperative contraction of the cells caused the backbone to bend and stretch in a walking motion, which traveled at a maximum speed of  $38 \mu\text{m s}^{-1}$ . Kim *et al.*<sup>5</sup> established a swimming microrobot by micro-molding PDMS. Using cardiomyocytes, cells were seeded on top of four conjoined cantilever beams that were grooved to

<sup>a</sup>Department of Bioengineering, University of Illinois at Urbana-Champaign, Urbana, Illinois, 61801, USA

<sup>b</sup>Department of Chemical and Biomolecular Engineering, University of Illinois at Urbana-Champaign, Urbana, Illinois, 61801, USA

<sup>c</sup>Department of Electrical and Computer Engineering, University of Illinois at Urbana-Champaign, Urbana, Illinois, 61801, USA

<sup>d</sup>Department of Mechanical Engineering, University of Illinois at Urbana-Champaign, Urbana, Illinois, 61801, USA

<sup>e</sup>2000 Micro and Nanotechnology Laboratory, MC-249, University of Illinois at Urbana-Champaign, 208 North Wright Street, Urbana, Illinois, 61801, USA. E-mail: rbashir@illinois.edu; Fax: +1 (217) 244-6375; Tel: +1 (217) 333-3097

† Electronic supplementary information (ESI) available. See DOI: 10.1039/c1lc20688e

influence the alignment and enhance their contractility relative to flat beams. An increase in force (88%) and bending (40%) was recorded, with an average swimming speed of  $140 \mu\text{m s}^{-1}$ . Feinberg *et al.*<sup>6</sup> assembled cardiomyocytes on various PDMS thin films with proteins to create muscular thin films. When released, these thin films curled or twisted into 3D conformations that purportedly performed gripping, pumping, walking ( $133 \mu\text{m s}^{-1}$ ), and swimming functions ( $400 \mu\text{m s}^{-1}$ ).

However, progress in developing cell-based biohybrid actuators has been limited to rigid materials, ranging in elastic moduli on the order of mega ( $10^6$ ) to giga ( $10^9$ ) Pascals. Recent reports in the literature have established a correlation between substrate rigidity and its influence on the contractile behavior of cardiomyocytes.<sup>1,2,10,11</sup> These studies show that cardiomyocytes cultured on hard substrates overstrain themselves, lack striated myofibrils, and stop beating. Conversely, substrates showing a close correspondence to tissue elasticity ( $\sim 10$  kPa) are optimal for transmitting contractile work to the substrate and for longer periods of time.<sup>1</sup> Therefore, it is worthwhile to explore and evaluate more compliant cantilevers with tissue-like elasticity on the order of kilo ( $10^3$ ) Pascals, and subsequently measure the contractile stresses and forces of cardiomyocytes on these devices.

While its mechanical properties can easily be altered in the kilo ( $10^3$ ) Pascal range<sup>12–14</sup> by changing the monomer-to-curing agent mixing ratio, functionalization of PDMS-based substrates for cell adhesion is challenging.<sup>15</sup> This can be attributed to its chemical inertness, hydrophobicity, and high chain mobility. In particular, chain mobility is probably the key limiting factor in modifying PDMS; surface treatments lead to unstable and short-lived oxidized layers.<sup>16</sup> Thus, physical adsorption is relatively inefficient and transient on PDMS. Furthermore, PDMS-based microfabrication requires master molds patterned by photolithography with SU-8 photoresist and silicon. This conventional photolithography process requires clean room facilities and costly equipment, which limits the complexity of multi-layer constructs and the ability to make changes quickly and cheaply.

In contrast, poly(ethylene glycol) (PEG) is a synthetic polymer that has tissue-like elasticity, which can be fine-tuned by changing its molecular weight or percent composition.<sup>17</sup> PEG-based hydrogels are hydrophilic and can be functionalized by activating with Sulfo-SANPAH and conjugating with full-length ECM molecules.<sup>18</sup> Cell adhesion domains,<sup>19,20</sup> growth factors,<sup>21</sup> and hydrolytic<sup>22</sup> and proteolytic sequences<sup>23,24</sup> can also be incorporated directly into the PEG backbone. Additionally, PEG is highly permeable to oxygen, nutrients, and other water-soluble metabolites. This is especially advantageous for cell-encapsulated, three-dimensional (3D) model systems. PEG-based hydrogels can be photopolymerized with a UV laser or lamp based on 3D CAD images; thus, complex 3D geometries can be formed through direct exposure.

This study uses a 3D stereolithographic printer to rapidly fabricate multi-material hydrogel cantilevers with varying stiffness. A stereolithography apparatus (SLA) is a rapid prototyping tool<sup>25,26</sup> used to produce three-dimensional (3D) models, prototypes, and patterns by repetitive deposition and processing of individual layers.<sup>27,28</sup> It uses a UV laser (325 nm) to directly write on and polymerize photosensitive liquid materials based on a CAD-designed digital blueprint, sliced into a collection of

two-dimensional (2D) cross-sectional layers, and processed into a real 3D part using layer-by-layer deposition. The automated, high-throughput process is particularly useful for biohybrid systems due to its multi-material capability, which can be used to change the synthetic material composition or insert cells or proteins at precise locations on the structure.<sup>29</sup> It has recently been adapted for use with photopolymerizable hydrogels,<sup>30,31</sup> which are highly hydrated and crosslinked polymer networks. The SLA is particularly useful for testing biohybrid actuator designs because of the ease in changing the dimension and shapes quickly and producing new ones to seed cardiomyocytes on. The aim of this paper is to incorporate acrylic-PEG-collagen into photopolymerizable PEGDA hydrogels (PEGDA-PC) to create cantilevers in the SLA that can be used to measure contractile forces at different stiffnesses and to see how those stiffnesses affect the contractility of cardiomyocytes for the design of cell-based biohybrid actuators.

## Materials and methods

### Apparatus and preparation of pre-polymer solution

A commercial stereolithography apparatus (SLA, Model 250/50, 3D Systems, Rock Hill, SC, USA) was modified for the fabrication of biohybrid cantilevers. The modification employed an additive “bottom-up” method as previously described.<sup>31</sup> The laser wavelength was in the UV-A region (325 nm) with a  $250 \mu\text{m}$  beam diameter at the set focal plane. The platform had a minimum Z-step of  $50 \mu\text{m}$ . Acrylic-PEG-collagen was prepared by mixing a working solution of acrylic-PEG-NHS ( $50 \text{ mg mL}^{-1}$  in ice cold HBSS) with collagen I ( $3.68 \text{ mg mL}^{-1}$ , rat tail; BD Biosciences) at a 1 : 1 acryl-to-lysine molar ratio for 30 minutes at  $4^\circ\text{C}$ . A 50% (v/v) acrylic-PEG-collagen solution was mixed with 20% poly(ethylene glycol) diacrylate (PEGDA) and 0.5% Irgacure 2959 photoinitiator in ice cold HBSS to form the pre-polymer solution. The PEGDA molecular weight ( $M_w$ ) was varied to fabricate the base ( $M_w$  700 Daltons) and beam (either  $M_w$  700 or  $M_w$  3400 Daltons) of the cantilevers. PEGDA was purchased from Sigma-Aldrich ( $M_w$  700 Daltons) and Laysan Bio ( $M_w$  3400 Daltons). A working solution of Irgacure 2959 photoinitiator (Ciba, Basel, Switzerland), which is only partially water-soluble, was prepared at 50% (w/v) by dissolution in DMSO.

### Fabrication of multi-material biopolymer cantilevers

To prepare for use in the SLA, energy dose characterizations of the pre-polymer solutions were performed using a method described previously.<sup>31</sup> Briefly, the pre-polymer solutions were pipetted into small containers capped on top by thin cover glasses. The SLA laser was used to draw circles that were 1 cm in diameter through the cover glass. The energy dose was varied by changing the scan speeds of the laser, which produced cylindrical gels of different thicknesses attached to the cover glasses. The thicknesses of these gels were measured and a working curve was plotted to determine the penetration depth ( $D_p$ ) and critical exposure energy ( $E_c$ ) of the pre-polymer solution necessary to produce cantilever beams with precise thicknesses. It was also observed that a change in the energy dose affected the elastic modulus of the gels. As a result, a constant energy dose



(150 mJ cm<sup>-2</sup>) was used to polymerize both the PEGDA-PC 700 and 3400 cantilever beams so that only the  $M_w$  of the hydrogels would affect the elastic modulus.

The fabrication setup consisted of a 35 mm diameter Petri dish and an 18 × 18 mm cover glass that was bonded to the dish with double-sided tape. The dish was positioned at the center of the SLA platform, and a carefully characterized volume of pre-polymer solution was added into it. The beam of the cantilever was fabricated first, by selective laser crosslinking of the pre-polymer solution, to ensure the precise thickness was not affected by the energy dose. The unpolymerized solution was then evacuated using a pipette and an equal volume of the pre-polymer solution for the cantilever base was added. The SLA then polymerized the first layer of the base (300 μm thick) according to the characterized energy dose for PEGDA-PC 700. The pre-polymer solution was added, and the elevator controlled by the SLA was lowered to a specified distance. After photopolymerization, the part was recoated, and the process was repeated until completion. In all, the fabrication of the cantilevers took not more than 15 minutes, although the processing time can be accelerated. The cantilevers were then transferred to a 0.02 N acetic acid solution to be washed. This step prevented the high collagen concentration in the unpolymerized pre-polymer solution from gelling around the cantilever; however, this step should only be done for less than a minute as acetic acid affects cardiomyocyte adhesion on the polymerized collagen from the cantilever beams. After washing out the pre-polymer solution, the cantilevers were moved to a physiological pH buffer solution to swell overnight. A total of 4 cantilevers were fabricated in one run, but the SLA process can easily be scaled up to accommodate many more.

### Cardiomyocyte isolation and culture

The warm growth medium consisting of Dulbecco's modified Eagle's medium (DMEM) and 10% fetal bovine serum (FBS) was prepared for cell culture. Cardiomyocytes were obtained from 2 day old neonatal Sprague-Dawley rats (Harlan Laboratories) using an approved protocol by the Institutional Animal Care and Use Committee (IACUC; Protocol #08190). Briefly, whole hearts were excised from the rats as described by Maass and Buvoli,<sup>32</sup> and placed in an ice-cold HBSS buffer. Using small scissors, the left and right atria were removed and the remaining ventricles were minced into 1 mm<sup>3</sup> pieces. The minced ventricles were digested in 0.1% (w/v) purified trypsin (Worthington Biochemicals), while gently rocking at 4 °C overnight. After 18 hours, warm growth medium was added for 5 minutes at 37 °C to inhibit trypsin digestion. The supernatant was discarded, and 0.1% (w/v) purified type II collagenase (Worthington Biochemicals) was added for 45 minutes while gently rocking at 37 °C. The digested tissue was triturated to mechanically loosen the cells, and the suspension was filtered through a 75 μm cell strainer to remove undigested connective tissue. The suspension was removed after centrifugation at 150 × *g* for 5 minutes. The remaining cell pellet was re-suspended in warm growth medium and pre-plated for 1 hour to enrich the suspension for cardiomyocytes. The cardiomyocytes were then counted and seeded on the backside of the cantilevers. To do this, individual cantilevers were placed in a 24-well plate, turned upside down, and evacuated of all liquid. They were allowed to dry for 10 min so

that the cantilevers would temporarily attach to the bottom of the dish. The cantilevers were then seeded at 2 million cells per well (1 × 10<sup>6</sup> cells cm<sup>-2</sup>) and incubated for 12 hours. After cell attachment, the cantilevers were transferred to a new dish with fresh medium and cultured overnight.

### Hydrogel characterization

The stiffness of a gel disk fabricated in the SLA was evaluated by measuring the elastic modulus ( $E$ ) using a mechanical testing system (Insight, MTS Systems, Eden Prairie, MN, USA). The gel disk with a diameter of 5 mm was compressed at a constant deformation rate of 1.0 mm s<sup>-1</sup> at 25 °C, and the resulting stress was recorded by MTS software (Testworks 4). From the strain limit to the first 10%, the elastic modulus was calculated using the slope of the stress ( $\sigma$ ) vs. strain ( $\lambda$ ) curve.

The swelling ratios of the gels at equilibrium were determined by measuring the weight of the swollen gels after 24 hours in pH 7.4 buffer solutions at 37 °C and the weight of the dried gels. The degree of swelling ( $Q$ ), defined as the reciprocal of the volume fraction of a polymer in a gel ( $v_2$ ), was calculated from the following equation:

$$Q = v_2^{-1} = \rho_P \left( \frac{Q_m}{\rho_S} + \frac{1}{\rho_P} \right)$$

where  $\rho_S$  was the density of water,  $\rho_P$  was the density of polymer, and  $Q_m$  was the swelling ratio, the mass ratio of the swelled gel to the dried gel.

### Experimental setup for measuring cantilever bending angles

Vertical motion and bending angles of the cantilevers due to cardiomyocyte cell sheet contraction were captured using a camcorder (HandyCam, Sony USA, New York, NY USA) with an advanced HAD CCD imager at 720 × 480 pixel video capture resolution. The camcorder recorded at 60 fps with a 60× optical zoom. It was fixed on a multi-axis stage (Thorlabs) and placed in a temperature- and CO<sub>2</sub>-controlled culture chamber due to cardiomyocyte sensitivity to changes in the outside environment. The temperature and CO<sub>2</sub> were set to 37 °C and 5%, respectively. The bending angles,  $\theta$ , and deflection values,  $\delta$ , were measured using the Measure Tool in Adobe Photoshop software (Fig. S1†). Still images were taken by the camcorder, and a line was fitted along the slope of the free end of the deformed cantilever. A second line was drawn along the horizontal axis of the undeformed cantilever, which created a protractor for measuring the angle. The vertical distance of the cantilever from the undeformed base to its deformed base was also measured to determine the deflection value. The smallest resolution that could be measured with this software platform was 0.1°.

### Modeling and analysis methods

Modeling and analysis of the cell-based biohybrid cantilevers were carried out using an analytical solution based on finite element modeling (FEM) analysis and validated by classical beam equations. FEM is a powerful technique when used to find numerical solutions to problems with irregular geometries or nonlinear material behavior. This is especially the case for cantilevers in which the beam width cannot be ignored. The

intrinsic stress calculations were validated using the following equation:<sup>33</sup>

$$\sigma_{\text{beam}} = \frac{2E_b \delta t_b}{L^2}$$

where  $\sigma_{\text{beam}}$  is the intrinsic stress (Pa),  $E_b$  is the elastic modulus of the beam,  $\delta$  is the deflection of the beam (m),  $t_b$  is the thickness of the beam (m), and  $L$  is the length of the beam (m) (Fig. S2†).

Cells seeded on the cantilevers formed sheets that were considered thin films, and the cantilevers were modeled as composite, two-component systems. The model was validated by simulating cantilevers with beam dimensions and comparing the stress calculations to Atkinson's approximation, a variant of Stoney's equation:<sup>8</sup>

$$\sigma_{\text{film}} \approx \frac{\delta E_b t_b^3}{4t_f(1-\nu_b)(t_f + t_b)L}$$

where  $\sigma_{\text{film}}$  is the cell sheet stress (Pa),  $t_f$  is the thickness of the cell sheet (m), and  $\nu_b$  is Poisson's ratio of the beam (Fig. S3†).

The simulations were performed with measured elastic moduli of 503 kPa for PEGDA-PC 700 and 17.82 kPa for PEGDA-PC 3400. Poisson's ratio of PEGDA-PC was assumed to be 0.499. Based on the literature, the elastic modulus of a sheet of cardiomyocytes was assumed to be 10 kPa with a thickness of 10  $\mu\text{m}$ .<sup>34,35</sup> The density of cardiomyocytes and the PEGDA-PC material was assumed to be 1.06  $\text{kg m}^{-3}$  and 1.12  $\text{kg m}^{-3}$ , respectively.

### Immunostaining

Cells seeded on cantilevers after 3 days were washed twice with HBSS and fixed in 4% (v/v) formaldehyde solution for 10 minutes at room temperature. The cantilever beams were physically detached from their bases with a sharp razor. The beams were permeabilized in 0.2% (v/v) Triton-X 100 in HBSS for 10 minutes at room temperature. The samples were washed twice with HBSS before a blocking agent, Signal FX (Invitrogen), was added for 30 minutes. After another wash step, the samples were incubated overnight at 4 °C with primary antibodies, mouse anti- $\alpha$ -actinin (sarcomeric) and rabbit anti-connexin-43. The tissues were washed twice before being incubated with Alexa Fluor 488 goat anti-mouse and Alexa Fluor 594 goat anti-rabbit secondary antibodies for 2 hours at 37 °C. The stained samples were washed with HBSS and subsequently stained with an antibody for DNA, 4',6-diamidino-2-phenylindole (DAPI, Sigma Aldrich, St Louis, MO, USA) for 5 minutes. After a final wash step, the cells on the cantilevers were imaged using an inverted fluorescent microscope (IX81, Olympus, Center Valley, PA, USA).

## Results and discussion

### Cantilever fabrication

The cantilevers were fabricated using a PEGDA backbone that was chemically linked with acrylic-PEG-collagen (Fig. 1A). PEGDA is a tissue-like, synthetic hydrogel that can be cross-linked in the presence of a photoinitiator.<sup>36,37</sup> It is mechanically stable, and its properties can be tuned by varying the polymer molecular weight, percent composition, or laser energy dose. It was previously established that changing the molecular weight of

20% PEGDA from 700 to 10 000 Daltons and photopolymerizing it in the SLA could be used to modulate the elasticity from  $503 \pm 57$  kPa to  $4.73 \pm 0.46$  kPa, respectively.<sup>31</sup> Collagen was chemically linked to the PEGDA backbone by acrylating its lysines, making them photocrosslinkable. Because PEGDA is normally inert, the collagen served to promote cell adhesion to the cantilever beams. The addition of collagen to the PEGDA backbone did not noticeably affect the mechanical properties of the hydrogel. Both the elastic modulus (Fig. 1B) and swelling ratio (Fig. 1C) were conserved for PEGDA-PC 700 and 3400. For 20% PEGDA-PC 700, the elastic modulus was  $507 \pm 110$  kPa, and the swelling ratio was  $6.25 \pm 0.06$ . For 20% PEGDA-PC 3400, the elastic modulus was  $29.8 \pm 17$  kPa, and the swelling ratio was  $13.6 \pm 0.95$ . From a biological perspective, mechanical properties of these hydrogels are closer to the *in vivo* environment of cells than either silicon or PDMS. They are also optically transparent, and therefore force measurements and immunofluorescence imaging of specific biological markers can be made simultaneously under light microscopes.<sup>38,39</sup>

Eight cantilevers were built for every fabrication run, with two sharing a common base. The SLA setup (Fig. 2A) can be easily modified with a larger-sized container to scale up the number of cantilevers in each run. The original dimensions (length  $\times$  width  $\times$  thickness) for the cantilevers were specified in CAD-based software, with the bases being  $2 \times 2 \times 4$  mm and the cantilever beams being  $2 \times 4 \times 0.45$  mm (Fig. 2B). An inherent characteristic of PEGDA hydrogels, however, is its tendency to imbibe water and swell many times beyond its intended dimensions. The cantilever thickness had to be adjusted to account for this swelling. The actual dimensions of PEGDA-PC 700 and 3400 cantilevers after 24 hours of equilibrium swelling were  $4.1 \times 2.1 \times 0.45$  mm and  $4.3 \times 2.3 \times 0.45$  mm, respectively. One major benefit of the SLA approach is that more than one biomaterial, growth factor, or cell type can be introduced and spatially defined in the same 3D construct.<sup>40</sup> This is especially useful for creating gradients of varying mechanical or bioactive properties. In particular, cantilevers were fabricated on a base consisting of PEGDA 700. The beams themselves were exchanged for either PEGDA-PC 700 or 3400, depending on the desired elasticity. As shown in the simplified process flow (Fig. 2C), the cantilever beams were fabricated first in the SLA to ensure the correct thickness, while maintaining the laser energy dose ( $150 \text{ mJ cm}^{-2}$ ) between PEGDA-PC 700 and 3400 materials to preserve the same trend in elasticity. The resulting PEGDA-PC 700 (Fig. 3A) and PEGDA-PC 3400 (Fig. 3B) cantilevers are shown with comparable dimensions after equilibrium swelling in HBSS.

### Cantilever beam intrinsic stress

Following the fabrication phase, cantilevers were rinsed in 0.02 N acetic acid to remove unpolymerized material before soaking overnight in HBSS. The cantilever beams would initially bend downward due to the weight of the unpolymerized pre-polymer solution and begin to swell as water diffused into them. Over time, the cantilevers would reach an equilibrium swelling state and bending would resolve to a final angle. These angles were measured using ImageJ analysis software and converted to displacement values. It was found that as the average molecular weight of the PEG-based cantilevers increased, the bending angle

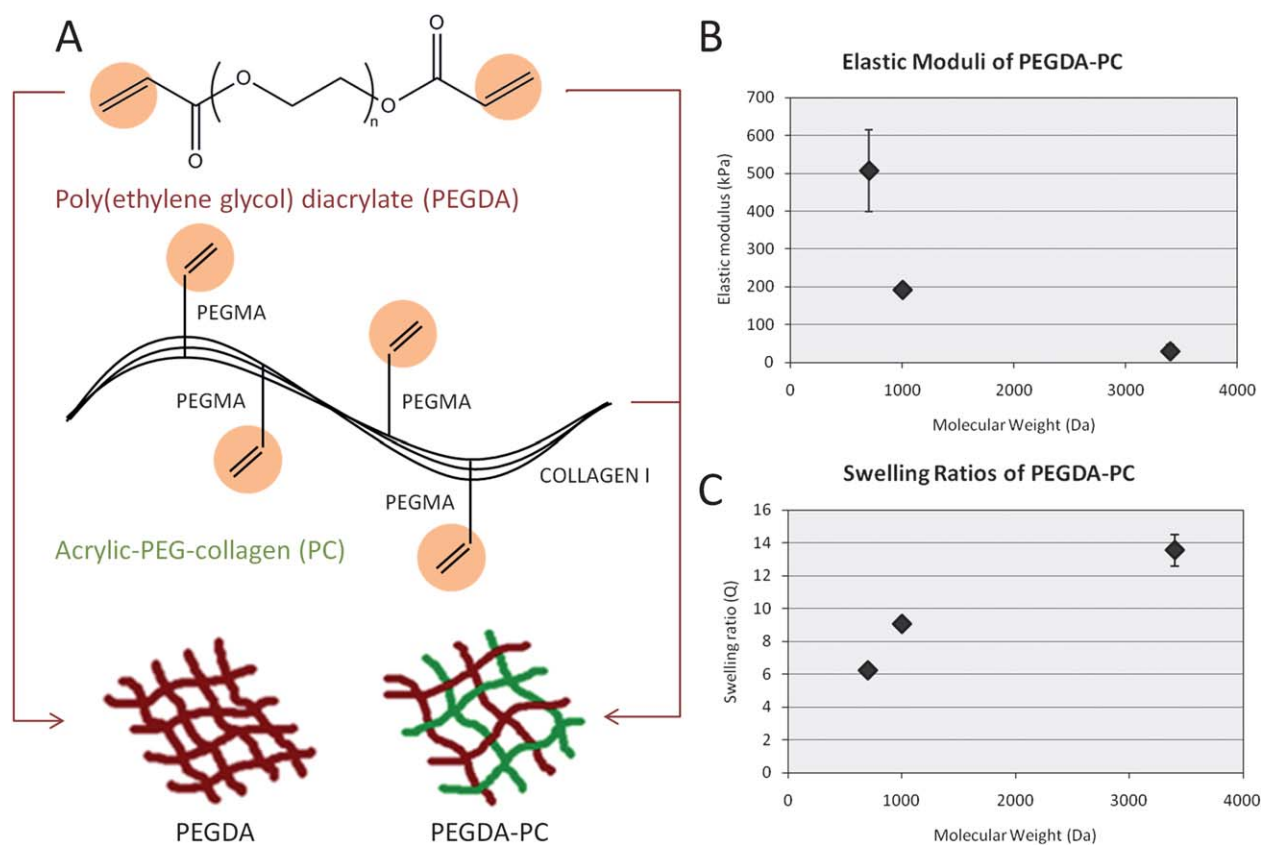


**Fig. 1** Biohybrid material. (A) A mixture consisting of poly(ethylene glycol) diacrylate (PEGDA) and acrylic-PEG-collagen (PC) was formulated as the photopolymerizable material for fabricating cantilever beams. Collagen I, extracted from rat tail, was modified on their lysine groups with acrylic groups to UV cross-link to the PEG backbone in the presence of a photoinitiator. (B and C) The mechanical properties of PEGDA-PC hydrogels were measured using a compression test at increasing molecular weight, demonstrating that the cantilever beams can be tuned to a wide range of elastic moduli and swelling ratios. These values did not change from that of PEGDA-only hydrogels, which suggests that the incorporation of acrylic collagen did not affect bulk mechanical properties. For  $n = 3$  and SD.

would increase upward in the clockwise direction. Similarly, the bending angle of the cantilevers would increase as the thickness of the cantilever decreased (Fig. S4†). PEGDA-PC 3400 had a bending angle of  $67.1 \pm 7.9^\circ$  ( $3420 \pm 560 \mu\text{m}$  deflection), whereas PEGDA-PC 700 did not bend ( $0^\circ$  angle and  $0 \mu\text{m}$  deflection).

Finite element analysis (COMSOL simulations) was used with the displacement values to calculate the intrinsic stress of the cantilever beams (Fig. 3C). The insets in Fig. 3C show the simulated displacement values, which were used to calculate the intrinsic stress for PEGDA-PC 700 and 3400. The intrinsic stresses obtained were  $0 \pm 0 \text{ Pa}$  and  $4160 \pm 910 \text{ Pa}$ , respectively.

One hypothesis for the cantilever bending due to non-uniform residual stress is that during the UV laser polymerization in the SLA, the highest concentration of energy is focused at the surface of the pre-polymer solution. As the laser penetrates into the solution, it is absorbed by the photoinitiator and monomers. By the time it reaches a penetration depth of  $450 \mu\text{m}$  at the other end of the beam, the energy is decreased, which reduces the overall crosslinking density. A simple calculation using the Beer-Lambert law reveals a 79.1% decrease in light transmittance ( $\lambda = 325 \text{ nm}$ ) through the pre-polymer solution at a depth of  $450 \mu\text{m}$  (see ESI†). This leads to a gradient in microstructure of the polymerized gel across the thickness. Consequently, the properties of the gel, such as swelling due to water absorption

and stiffness, also have a gradient. This gradient in swelling across the thickness causes bending of the cantilever.

### Cardiomyocyte adhesion and spreading

PEGDA hydrogels are hydrophilic and well-known to resist cell adhesion. Many groups have chemically modified them with proteins and peptide sequences to make them more amenable to cell attachment.<sup>19</sup> One of the most frequently used sequences with PEGDA is RGD (arginine-glycine-aspartic acid), which is found in numerous extracellular matrix proteins. However, several reports have suggested that while RGD peptides promote cardiomyocyte adhesion, they are unable to promote the signaling required for normal FAK expression and complete sarcomere formation in cardiomyocytes.<sup>41</sup> Sarin *et al.*<sup>42</sup> went further to demonstrate that RGD depressed the rate of contractile force by altering the myofilament activation process. Based on these findings, we sought to improve cardiomyocyte function by chemically attaching collagen molecules to PEGDA hydrogels. This chemistry was performed by the reaction of lysine amines on collagen to acrylate-PEG-NHS, which is an *N*-hydroxysuccinimidyl ester reactive to amines. The acrylate-PEG-collagen was then combined in solution with PEGDA to form a PEG-based hydrogel linked with bioactive collagen for cell adhesion.

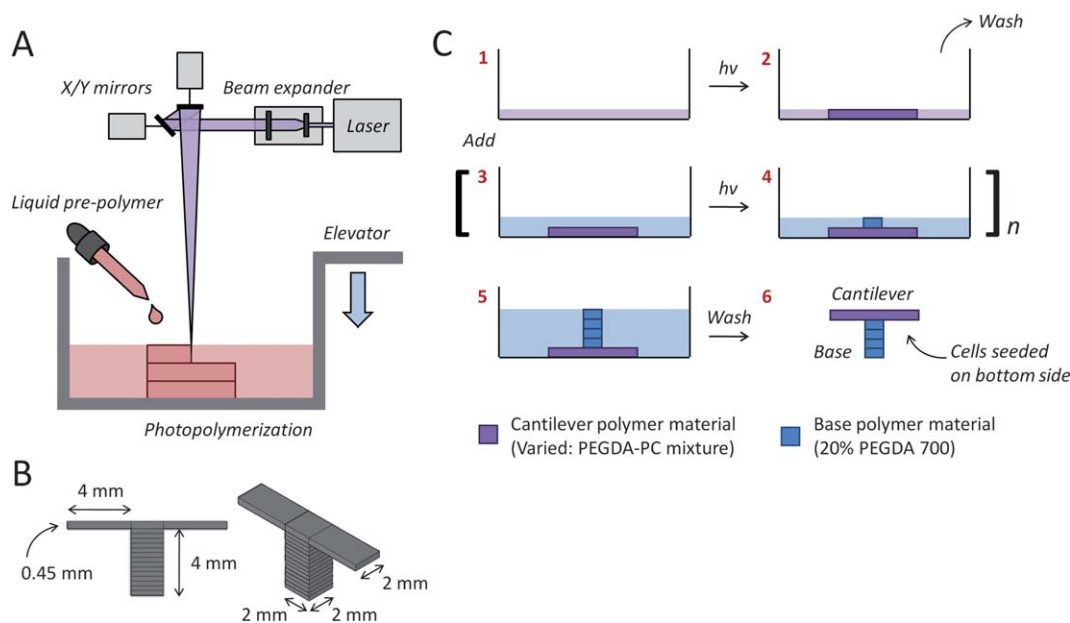


**Fig. 2** Multi-material cantilever fabrication. (A) The cantilevers were fabricated with a 3D stereolithographic printer, which uses a UV laser to construct layer-by-layer patterns. (B) Two separate cantilevers (2 mm wide  $\times$  4 mm long  $\times$  0.45 mm thick) were built on opposite ends of one base (2 mm wide  $\times$  2 mm long  $\times$  4 mm thick). The molecular weight of the PEGDA-PC cantilever beam was varied using either PEGDA-PC 700 or 3400, while the base was kept constant using PEGDA-PC 700. (C) A simplified fabrication process flow is shown, which begins with the formation of the cantilever beam before the base.

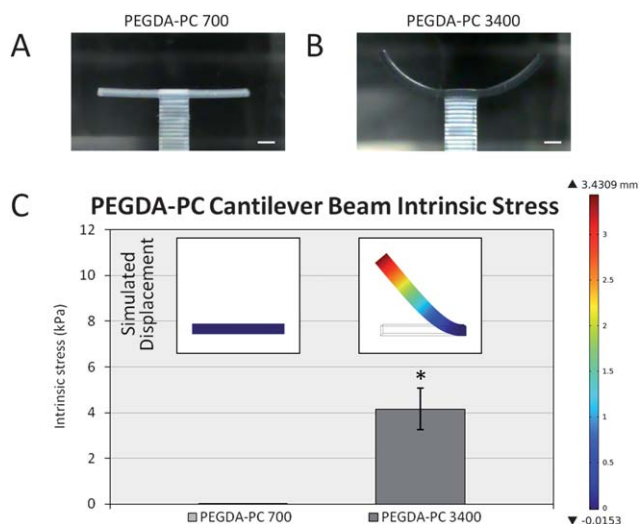


**Fig. 3** Intrinsic stress calculations. After the fabrication process, (A) PEGDA-PC 700 and (B) PEGDA-PC 3400 cantilevers were washed in HBSS to remove uncrosslinked pre-polymer solution. Due to an intrinsic stress, PEGDA-PC 3400 cantilevers would bend upward to relieve stress in the beams. (C) The peak stress was calculated by using finite element analysis to simulate the deflection of the cantilever beam (inset). Scale bars are 1 mm. Statistics by one-way ANOVA, Tukey's test,  $*p < 0.05$  for  $n = 8$  and SD.

Cardiomyocytes extracted from neonatal rat ventricular myocytes were seeded on PEGDA, PEGDA-RGD, and PEGDA-collagen (PEGDA-PC) hydrogels. After 2 days, cells were qualitatively evaluated for cell adhesion and spreading. It was clear that cardiomyocytes spread much better on PEGDA-

PC hydrogels than PEGDA and PEGDA-RGD (Fig. S5†). The cells on PEGDA and PEGDA-RGD appeared to remain balled up in spheres and preferentially attached to each other rather than on the substrate. Many of the cells had washed off after a change of media indicating poor cell attachment. On the other hand, cardiomyocytes on PEGDA-PC spread greatly, formed gap junctions, and began to contract in synchrony. Because of that, we used PEGDA-PC hydrogels as our material choice for cantilever fabrication, which has the bioactivity for cell attachment and function, and ability to change its mechanical stiffness through its molecular weight.

#### Cantilever bending due to cell traction forces

As a result of the intrinsic stress, the curvature of the PEGDA-PC 3400 cantilevers made it difficult to seed cells uniformly and at high densities on the beams. One solution was to turn the cantilevers on their back sides and evacuate the liquid they were immersed in. This created a surface tension that mechanically flattened the curved cantilever beams onto the bottom of the plate. Neonatal rat ventricular myocytes were then extracted and seeded on the flattened cantilever beams at 1 million cells  $\text{cm}^{-2}$ . This backside seeding also prevented the cell sheets on the two cantilevers from linking together, so that they could be examined as two independent measurements. The cantilevers with seeded cells were centrifuged to distribute cells evenly on the cantilevers.

After seeding, cardiomyocytes were allowed to adhere for 24 hours. By then, the cantilevers had already started to bend downward due to cell traction forces as the cardiomyocytes began to spread and reorganize themselves. Cell traction forces are generated by actomyosin interactions and actin polymerization, and regulated by intracellular proteins such as  $\alpha$ -smooth muscle



actin and soluble factors such as TGF- $\beta$ . Once transmitted to the extracellular matrix through stress fibers *via* focal adhesions, which are assemblies of ECM proteins, transmembrane receptors, and cytoplasmic structural and signaling proteins, cell traction forces direct many cellular functions, including cell migration, ECM organization, and mechanical signal generation. The stress induced by the cell sheet is clearly seen by the change in displacement over time on the cantilever beams (Fig. 4A). The cell sheet continued to apply traction forces on the cantilevers over 72 hours before it stabilized. The bending angle of the curved beams was measured and recorded every day for 4 days (Fig. 4B). Because of the cell traction forces, the bending angle for PEGDA-PC 3400 cantilevers was decreased from its intrinsic value of  $67.1 \pm 7.9^\circ$  to  $44.2 \pm 6.0^\circ$  by the third day of culture. PEGDA-PC 700 cantilevers, having a high elastic modulus, did not bend at all during culture. The displacement values were also measured and used in FEM simulations to calculate the stress on the cantilever beams by the cell sheet. The simulated displacements and stresses for PEGDA-PC 700 and 3400 are shown in Fig. 4C. For PEGDA-PC 3400, the highest level of stress was seen at the fixed end of the beam. The maximum stress values were calculated every day (Fig. 4D), and the change in stress was plotted every 24 hours. The cell sheet reached a maximum stress of 2040 Pa before it leveled off. The change in stress was highest after the first day and continually decreased before there was virtually no change between 72 and 96 hours.

### Cantilever actuation and force

Although cardiomyocytes began to contract individually as early as 24 hours after seeding, the cells did not beat synchronously as a whole sheet until at least 48 hours. During this period, cardiomyocytes formed electrical connections between each other through gap junctions. Membrane proteins known as connexins formed six-membered rings called connexons on the sarcolemma of cardiomyocytes. When gap junctions are open, they provide direct communication between the sarcoplasmic spaces of adjoining cells, creating a functional syncytium or network of synchronized cells.<sup>43,44</sup> After 76 hours, when the majority of these connections were formed, cells were stained for sarcomeric  $\alpha$ -actinin to qualitatively elucidate the morphology of cardiomyocytes on PEGDA-PC 700 and 3400 cantilevers (Fig. 5A). In both cases, cardiomyocytes exhibited the expression of sarcomeric  $\alpha$ -actinin, an actin-binding protein that plays a key role in the formation and maintenance of Z-lines, throughout the cytoskeleton. The localization of sarcomeric  $\alpha$ -actinin in both PEGDA-PC 700 and 3400 demonstrated a typical periodicity in the Z-lines of cardiomyocytes.

Actuation of the PEGDA-PC 700 and 3400 cantilevers is shown in Movies S1 and S2†. Actuation of the cantilevers is a consequence of the contraction and relaxation of the cardiomyocyte cell sheet through the sliding filament mechanism.<sup>45</sup> During contraction, cardiomyocyte filaments shorten by the

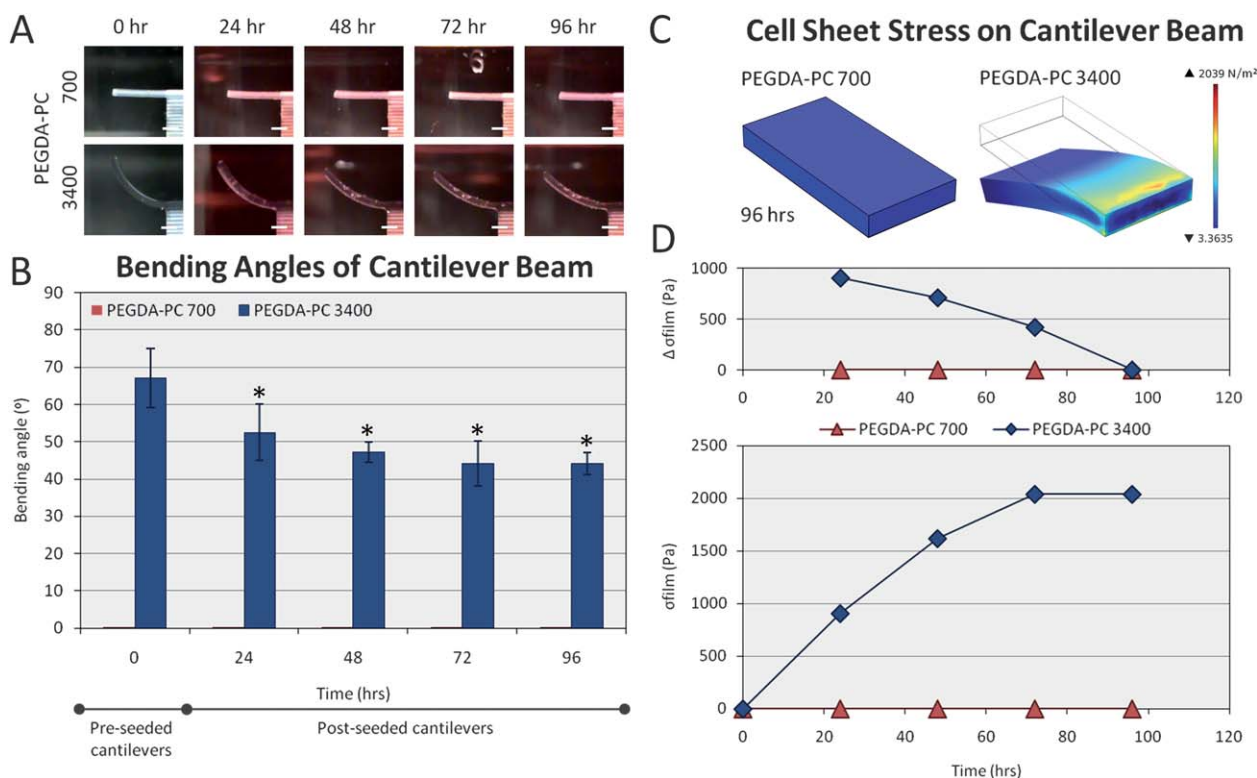


**Fig. 4** Cell sheet stress calculations. Cells from the ventricles of neonatal rat hearts were seeded on the backside of the cantilever beams. (A) The traction forces of these cells, which are responsible for migration, proliferation, and differentiation, caused the PEGDA-PC 3400 cantilever beams to deflect downward in the Z-direction over time. (B) The average bending angles of the cantilevers were measured over a 96 hour period, which was used to calculate the deflection at the tip of the beams. (C) These deflections were simulated using finite element analysis to calculate the stresses exerted by the cell sheets due to traction forces. (D) These stresses exerted by the cell sheet and modeled as a thin film were plotted over time. The change in stress over 24 hour time points decreased and reached 0 by 96 hours. Scale bars are 1 mm. Statistics by one-way ANOVA, Tukey's test, \* $p < 0.05$  for  $n = 8$  and SD.



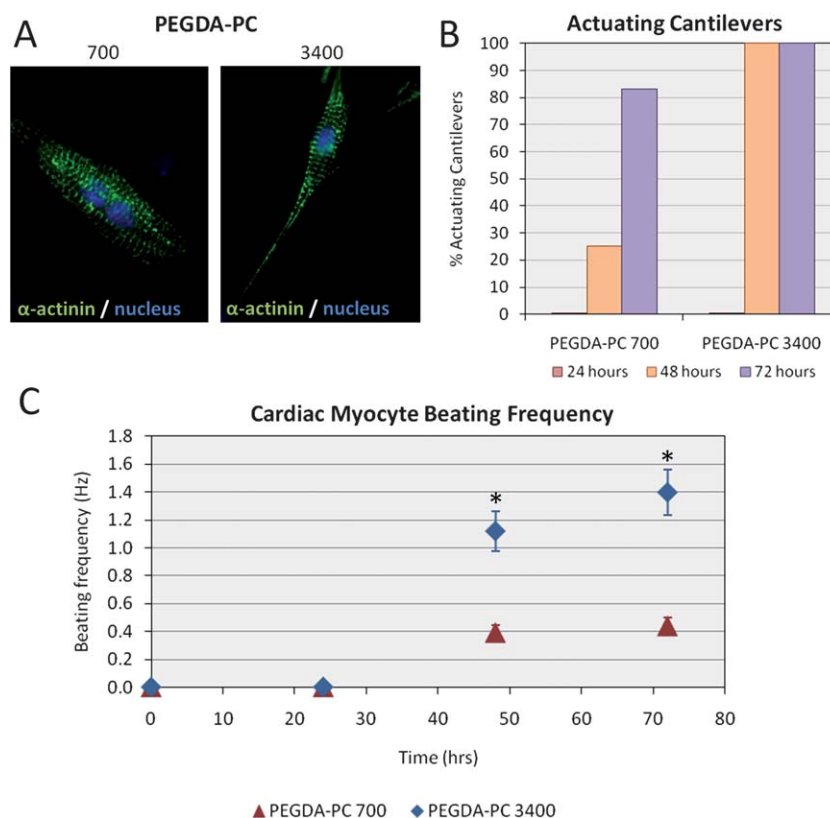


**Fig. 5** Cardiomyocytes on PEGDA-PC substrates. (A) Cells on the cantilevers were fluorescently labeled with anti-sarcomeric  $\alpha$ -actinin and anti-DNA. Qualitatively, cardiomyocytes on PEGDA-PC 3400 and PEGDA-PC 700 both expressed actomyosin complexes (striations), but those on PEGDA-PC 3400 appeared to be more elongated and spindle-shaped. (B) None of the PEGDA-PC cantilevers actuated until at least the second day in culture, but the number of actuating cantilevers on this day was much greater for PEGDA-PC 3400 than PEGDA-PC 700. (C) The beating frequency of the cardiomyocytes was also much greater for PEGDA-PC 3400 than PEGDA-PC 700, indicating a preference for the softer material. Statistics by one-way ANOVA, Tukey's test,  $*p < 0.05$  for  $n = 8$  and SD.

sliding of actin and myosin filaments in sarcomeres, as triggered by action potentials and intracellular calcium signals.<sup>46</sup> Calcium is the critical part of the medium that allows the actin, myosin, and ATP to interact, causing crossbridge formation and muscle contraction. This process continues as long as calcium is available to the actin and myosin. During relaxation, cardiomyocyte filaments return to their original position as calcium is pumped back into the sarcoplasmic reticulum, preventing interaction of the actin and myosin. Cardiomyocyte cell sheets on PEGDA-PC 3400 cantilevers had all started to actuate after 48 hours (100%), whereas only a quarter of the cardiomyocyte cell sheets on PEGDA-PC 700 cantilevers followed suit (25%) during the same time period (Fig. 5B). This percentage increased after 72 hours (83%), but the development of functional syncytium was clearly slower. Furthermore, the beating frequency of the cardiomyocyte cell sheet was greater for PEGDA-PC 3400 than 700. After 48 hours, cardiomyocytes on cantilever plates with  $M_w$  3400 reached a beating frequency of  $1.12 \pm 0.14$  Hz, while those for  $M_w$  700 reached  $0.39 \pm 0.05$  Hz, respectively (Fig. 5C). The frequency increased slightly for both after 72 hours to  $1.40 \pm 0.16$  Hz and  $0.44 \pm 0.06$  Hz, respectively. These results seem to be in agreement with previous reports that claim that the substrate elasticity of the developing myocardial microenvironment are optimal for transmitting contractile work to the matrix and for

promoting actomyosin striations.<sup>1</sup> In addition to the substrate elasticity, it is possible the hydrogels with higher molecular weight have more cell adhesive sites exposed on the surface of the cantilever than hydrogels with lower molecular weight.

Finally, we measured the actuation amplitudes of the cantilevers over 96 hours (Fig. 6A). Similar to the beating frequency, the amplitudes reached a maximum on the third day post-seeding with values of  $2 \pm 8 \mu\text{m}$  and  $390 \pm 40 \mu\text{m}$  for PEGDA-PC 700 and 3400, respectively. The actuation amplitudes did not reach a maximum suddenly; rather, they increased linearly over time as more cardiomyocytes joined the syncytium of cells. Using these amplitudes, we calculated the contractile forces of cardiomyocyte cell sheets on PEGDA-PC 700 and 3400 cantilevers by using the following equations (Fig. 6B):

$$F = k_c \delta$$

$$k_c = \frac{w}{4(E_f t_f + E_b t_b) L^3} \left( E_f^2 t_f^4 + E_b^2 t_b^4 + 4E_b t_b E_f t_f^3 + 6E_b t_b^2 E_f t_f^2 + 4E_b t_b^3 E_f t_f \right)$$

where  $F$  is the contractile force,  $k_c$  is the stiffness of the cantilever,  $w$  is the width of the beam, and  $E_f$  is the elastic modulus of the film. Stiffness,  $k_c$ , was derived for a composite, two-component system.<sup>47</sup> The stiffness values for PEGDA-PC 700 and 3400 were

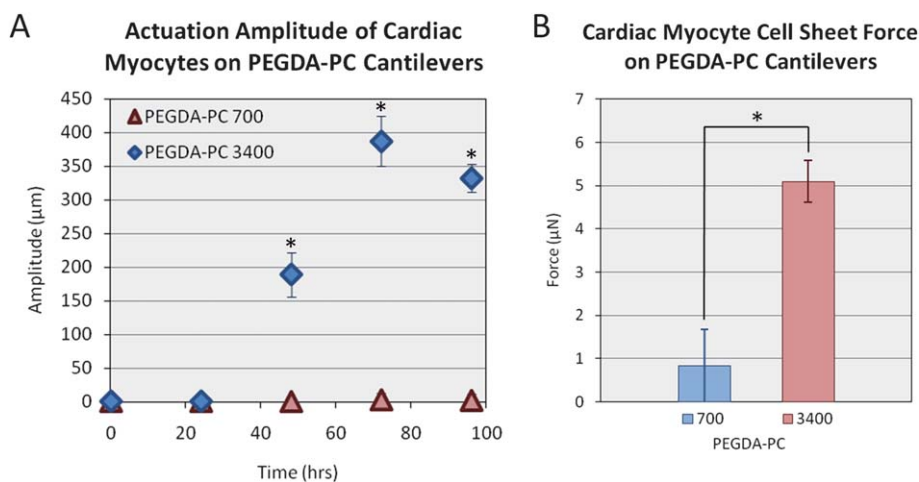


**Fig. 6** Force of contraction. Using an equation for cantilever beam stiffness, the force of contraction was calculated by multiplying the stiffness by the deflection of the cantilever after contraction. Statistics by one-way ANOVA, Tukey's test,  $*p < 0.05$  for  $n = 8$  and SD.

calculated to be  $0.36 \text{ N m}^{-1}$  and  $0.013 \text{ N m}^{-1}$ , respectively. Using these values, and the peak deflection of actuated cantilevers (from its relaxation state to its contraction state), the total calculated forces were  $0.89 \pm 2.89 \mu\text{N}$  for PEGDA-PC 700 and  $5.09 \pm 0.48 \mu\text{N}$  for PEGDA-PC 3400.

The mechanical forces generated with cardiomyocyte cell sheets on elastic substrates near that of the native myocardium can be used to model and design self-propelled bio-bots. There are several ways to improve the current output of force, such as aligning the cardiomyocytes by patterning proteins or grooves into the substrate.<sup>48</sup> The stiffness of the beam can be decreased by reducing the beam thickness or expanding its length. The density of cells can be increased by encapsulating them in 3D. Varying rigid (PEGDA-PC 700) and soft (PEGDA-PC 3400) materials throughout the bio-bot design can also be beneficial for maximizing deflection in one direction and minimizing it in another. These designs can be used to form the basis of more complex cell systems. For example, cardiomyocytes can later be replaced with skeletal myoblasts and co-cultured with neurons to form neuromuscular junctions. The genetic machinery of the neurons can be reprogrammed to form simple functions of switching on and off chemical secretions, which in turn can be used to stimulate muscle cells to propel the bio-bot. The advantage of using this hydrogel system over silicon and PDMS is that when we switch over to other cell types, which are sensitive to their environment, we can tune the elasticity of the substrate in accordance to them. As the stiffness is modulated for these specific cell types (*i.e.*, neurons and skeletal muscle cells), this may affect the curvature of the material due to cell traction forces, in which case more rigid materials can be used to maintain the structural integrity of the bio-bot. Thus, a true living, multi-cellular machine could be created using the capabilities of the SLA, which can perform multiple functions such as sensing, moving, and effecting.<sup>49</sup>

#### Control and longevity of cantilevers and actuators

The influence of various drug treatments has been evaluated on the contractile activity of cardiomyocytes.<sup>52</sup> For example, the

addition of isoproterenol to the medium can cause an increase in the contraction frequency, whereas the addition of carbamylcholine chloride to the medium can cause a decrease in the contraction frequency. Gap junction blockers, such as heptanol, can completely stop synchronous contractility. These effects are reversible; after 10 min in the drug-free culture medium, the synchronous beating of the cardiomyocytes was restored to its original amplitude and frequency. Pulsatile electrical stimulation can also be used to pace the contractions of cardiomyocytes.<sup>53</sup> Recently, light-induced stimulation of genetically engineered cardiomyocytes that express the light-activated cation channels, halorhodopsin or channelrhodopsin, was demonstrated.<sup>54,55</sup>

Experimentally, these cantilevers have been verified to function optimally for at least 5 days post-seeding. After this period, the frequency and amplitude of the actuating cantilevers decrease significantly. The lifetime of these cantilevers can be extended by reducing the overgrowth of fibroblasts in low serum medium.<sup>50</sup> Other groups have demonstrated up to 16 days of functional components with cardiomyocytes.<sup>6</sup> Furthermore, previous reported results on cardioids show that periods up to 60 days are readily attainable in culture.<sup>51</sup> Lifetimes beyond this would require new technologies to support long-term survival *in vitro*.

#### Conclusion

Multi-material cantilevers were fabricated using a 3D stereolithographic printer with a PEGDA backbone that was incorporated with acrylic-PEG-collagen. The SLA allows us to quickly and easily change the material and its properties in the same 3D construct, which we show here with PEGDA-PC 700 and 3400 cantilevers. Cardiomyocytes were extracted and seeded on the backside of the cantilevers and cultured to form cell sheets. Through its traction forces, the cardiomyocytes created a stress on the cantilever, causing it to bend. These stresses were modeled using finite element analysis by mimicking the displacement of the cantilevers. For PEGDA-PC 3400, the maximum stress was 2040 Pa, while there was no stress on PEGDA-PC 700 because of its high stiffness. The cardiomyocytes then began to beat in synchrony after two days in

culture, and the contractile forces were calculated. The peak contractile forces were  $0.89 \pm 2.89 \mu\text{N}$  for PEGDA-PC 700 and  $5.09 \pm 0.48 \mu\text{N}$  for PEGDA-PC 3400. The stresses and forces calculated here can be used to design and optimize a cell-based biohybrid actuator that can generate net motion. The cantilevers can be used as an early prototype for the design and optimization of cell-based biohybrid actuators.

## Acknowledgements

This project was funded by the National Science Foundation (NSF), Science and Technology Center (STC) and Emerging Behaviors in Integrated Cellular Systems (EBICS) Grant CBET-0939511 (R.B., T.S., and H.K.) and by a cooperative agreement that was awarded to UIUC and administered by the U.S. Army Medical Research & Materiel Command (USAMRMC) and the Telemedicine & Advanced Technology Research Center (TATRC), under Contract #: W81XWH0810701.

## References

- 1 A. J. Engler, C. Carag-Krieger, C. P. Johnson, M. Raab, H. Y. Tang and D. W. Speicher, *et al.*, Embryonic cardiomyocytes beat best on a matrix with heart-like elasticity: scar-like rigidity inhibits beating, *J. Cell Sci.*, 2008, **121**(Pt 22), 3794–3802.
- 2 P. Bajaj, X. Tang, T. A. Saif and R. Bashir, Stiffness of the substrate influences the phenotype of embryonic chicken cardiomyocytes, *J. Biomed. Mater. Res., Part A*, 2010, **95A**(4), 1261–1269.
- 3 D. E. Discher, P. Janmey and Y. Wang, Tissue cells feel and respond to the stiffness of their substrate, *Science*, 2005, **310**(5751), 1139–1143.
- 4 J. Xi, J. J. Schmidt and C. D. Montemagno, Self-assembled microdevices driven by muscle, *Nat. Mater.*, 2005, **4**(2), 180–184.
- 5 J. Kim, J. Park, S. Yang, J. Baek, B. Kim and S. H. Lee, *et al.*, Establishment of a fabrication method for a long-term actuated hybrid cell robot, *Lab Chip*, 2007, **7**(11), 1504–1508.
- 6 A. W. Feinberg, A. Feigel, S. S. Shevkopyas, S. Sheehy, G. M. Whitesides and K. K. Parker, Muscular thin films for building actuators and powering devices, *Science*, 2007, **317**(5843), 1366–1370.
- 7 E. Choi, S. Q. Lee, T. Y. Kim, H. Chang, K. J. Lee and J. Park, MEMS-based power generation system using contractile force generated by self-organized cardiomyocytes, *Sens. Actuators, B*, 2010, **151**(1), 291–296.
- 8 K. Wilson, M. Das, K. J. Wahl, R. J. Colton and J. Hickman, Measurement of contractile stress generated by cultured rat muscle on silicon cantilevers for toxin detection and muscle performance enhancement, *PLoS One*, 2010, **5**(6), e11042.
- 9 J. Park, J. Ryu, S. K. Choi, E. Seo, J. M. Cha and S. Ryu, *et al.*, Real-time measurement of the contractile forces of self-organized cardiomyocytes on hybrid biopolymer microcantilevers, *Anal. Chem.*, 2005, **77**, 6571–6580.
- 10 J. G. Jacot, A. D. McCulloch and J. H. Omens, Substrate stiffness affects the functional maturation of neonatal rat ventricular myocytes, *Biophys. J.*, 2008, **95**(7), 3479–3487.
- 11 X. Tang, P. Bajaj, R. Bashir and T. A. Saif, How far cardiac cells can see each other mechanically, *Soft Matter*, 2011, **7**(13), 6151–6158.
- 12 S. Ikeda, F. Arai, T. Fukuda, E. H. Kim, M. Negoro and K. Irie, *et al.*, *In vitro* Patient-tailored Anatomical Model of Cerebral Artery for Evaluating Medical Robots and Systems for Intravascular Neurosurgery, 2005 *IEEE/RSJ International Conference on Intelligent Robots and Systems*, 2005, pp. 1558–1563.
- 13 D. Armani, C. Liu and N. Aluru, Re-configurable Fluid Circuits by PDMS Elastomer Micromachining, 12th *IEEE International Conference on Micro Electro Mechanical Systems, MEMS '99*, 1999, pp. 222–227.
- 14 X. Q. Brown, K. Ookawa and J. Y. Wong, Evaluation of polydimethylsiloxane scaffolds with physiologically-relevant elastic moduli: interplay of substrate mechanics and surface chemistry effects on vascular smooth muscle cell response, *Biomaterials*, 2005, **26**(16), 3123–3129.
- 15 A. Khademhosseini, *Micro and Nanoengineering of the Cell Microenvironment: Technologies and Applications*, Artech House, Boston, 2008.
- 16 J. Y. Wong, J. B. Leach and X. Q. Brown, Balance of chemistry, topography, and mechanics at the cell-biomaterial interface: issues and challenges for assessing the role of substrate mechanics on cell response, *Surf. Sci.*, 2004, **570**, 119–133.
- 17 J. L. Ifkovits and J. A. Burdick, Review: photopolymerizable and degradable biomaterials for tissue engineering applications, *Tissue Eng.*, 2007, **13**(10), 2369–2385.
- 18 S. R. Peyton, C. B. Raub, V. P. Keschrumrus and A. J. Putnam, The use of poly(ethylene glycol) hydrogels to investigate the impact of ECM chemistry and mechanics on smooth muscle cells, *Biomaterials*, 2006, **27**(28), 4881–4893.
- 19 D. L. Hern and J. A. Hubbell, Incorporation of adhesion peptides into nonadhesive hydrogels useful for tissue resurfacing, *J. Biomed. Mater. Res.*, 1998, **39**, 266–276.
- 20 B. K. Mann, A. S. Gobin, A. T. Tsai, R. H. Schmedlen and J. L. West, Smooth muscle cell growth in photopolymerized hydrogels with cell adhesive and proteolytically degradable domains: synthetic ECM analogs for tissue engineering, *Biomaterials*, 2001, **22**, 3045–3051.
- 21 E. A. Phelps, N. Landazur, P. M. Thule, R. Taylor and A. J. Garcia, Bioartificial matrices for therapeutic vascularization, *Proc. Natl. Acad. Sci. U. S. A.*, 2010, **107**(8), 3323–3328.
- 22 A. T. Metters, K. S. Anseth and C. N. Bowman, Fundamental studies of a novel, biodegradable PEG-*b*-PLA hydrogel, *Polymer*, 2000, **41**, 3993–4004.
- 23 J. L. West and J. A. Hubbell, Polymeric biomaterials with degradation sites for proteases involved in cell migration, *Macromolecules*, 1999, **32**, 241–244.
- 24 G. P. Raeber, M. P. Lutolf and J. A. Hubbell, Molecularly engineered PEG hydrogels: a novel model system for proteolytically mediated cell migration, *Biophys. J.*, 2005, **89**, 1374–1388.
- 25 S. M. Peltola, F. P. W. Melchels, D. W. Grijpma and M. Kellomaki, A review of rapid prototyping techniques for tissue engineering purposes, *Ann. Med.*, 2008, **40**(4), 268–280.
- 26 T. Burg, C. A. P. Cass, R. Groff, M. Pepper and K. J. L. Burg, Building off-the-shelf tissue-engineered composites, *Philos. Trans. R. Soc. London, Ser. A*, 2010, **368**(1917), 1839–1862.
- 27 F. P. W. Melchels, J. Feijen and D. W. Grijpma, A review on stereolithography and its applications in biomedical engineering, *Biomaterials*, 2010, **31**(24), 6121–6130.
- 28 H. Nguyen, J. Richter and P. F. Jacobs, On Windowpanes and Christmas Trees: Diagnostic Techniques for Improved Part Accuracy, in *Proc. 1st Eur. Conf. Rapid Prototyping*, ed. P. M. Dickens, University of Nottingham, Nottingham, 1992, pp. 133–161.
- 29 K. Arcaute, B. K. Mann and R. B. Wicker, Stereolithography of spatially controlled multi-material bioactive poly(ethylene glycol) scaffolds, *Acta Biomater.*, 2010, **6**(3), 1047–1054.
- 30 K. Arcaute, B. K. Mann and R. B. Wicker, Stereolithography of three-dimensional bioactive poly(ethylene glycol) constructs with encapsulated cells, *Ann. Biomed. Eng.*, 2006, **34**(9), 1429–1441.
- 31 V. Chan, P. Zorlutuna, J. H. Jeong, H. Kong and R. Bashir, Three-dimensional photopatterning of hydrogels using stereolithography for long-term cell encapsulation, *Lab Chip*, 2010, **10**(16), 2062–2070.
- 32 A. H. Maass and M. Buvoli, Cardiomyocyte preparation, culture, and gene transfer, *Methods Mol. Biol.*, 2007, **366**, 321–330.
- 33 S. D. Senturia, *Microsystem Design*, Springer, New York, 2000.
- 34 X. Shi, L. Qin, X. Zhang, K. He, C. Xiong and J. Fang, *et al.*, Elasticity of cardiac cells on the polymer substrates with different stiffness: an atomic force microscopy study, *Phys. Chem. Chem. Phys.*, 2011, **13**, 7540–7545.
- 35 M. F. Berry, A. J. Engler, Y. J. Woo, T. J. Pirolli, L. T. Bish and V. Jayasankar, *et al.*, Mesenchymal stem cell injection after myocardial infarction improves myocardial compliance, *Am. J. Physiol.*, 2006, **290**, H2196–H2203.
- 36 J. P. Fisher, D. Dean, P. S. Engel and A. G. Mikos, Photoinitiated polymerization of biomaterials, *Annu. Rev. Mater. Res.*, 2001, **31**, 171–181.
- 37 K. T. Nguyen and J. L. West, Photopolymerizable hydrogels for tissue engineering applications, *Biomaterials*, 2002, **23**(22), 4307–4314.
- 38 J. Rajagopalan and M. T. A. Saif, MEMS sensors and microsystems for cell mechanobiology, *J. Micromech. Microeng.*, 2011, **21**, 1–11.



- 39 K. A. Addae-Mensah and J. P. Wikswo, Measurement techniques for cellular biomechanics *in vitro*, *Exp. Biol. Med.*, 2008, **233**(7), 792–809.
- 40 P. Zorlutuna, J. H. Jeong, H. Kong and R. Bashir, Stereolithography-based hydrogel microenvironments to examine cellular interactions, *Adv. Funct. Mater.*, 2011, **21**(19), 3642–3651.
- 41 S. Y. Boateng, S. S. Lateef, W. Mosley, T. J. Hartman, L. Hanley and B. Russell, RGD and YIGSR synthetic peptides facilitate cellular adhesion identical to that of laminin and fibronectin but alter the physiology of neonatal cardiomyocytes, *Am. J. Physiol. Cell Physiol.*, 2005, **288**, C30–C38.
- 42 V. Sarin, R. D. Gaffin, G. A. Meininger and M. Methuchamy, Arginine-glycine-aspartic acid (RGD)-containing peptides inhibit the force production of mouse papillary muscle bundles *via* alpha 5 beta 1 integrin, *J. Physiol.*, 2005, **564**(Pt 2), 603–617.
- 43 N. J. Severs, A. F. Bruce, E. Dupont and S. Rothery, Remodeling of gap junctions and connexin expression in diseased myocardium, *Cardiovasc. Res.*, 2008, **80**(1), 9–19.
- 44 M. Noorman, M. A. van der Heyden, T. A. van Veen, M. G. Cox, R. N. Hauer and J. M. de Bakker, *et al.*, Cardiac cell–cell junctions in health and disease: electrical *versus* mechanical coupling, *J. Mol. Cell. Cardiol.*, 2009, **47**(1), 23–31.
- 45 M. D. Berne, M. N. Levy and B. M. Koeppen, *Physiology*, Mosby, St Louis, 2003.
- 46 M. W. Curtis and B. Russell, Micromechanical regulation in cardiac myocytes and fibroblasts: implications for tissue remodeling, *Eur. J. Physiol.*, 2011, **462**, 105–117.
- 47 W. Y. Shih, X. Li, H. Gu, W. Shih and I. A. Aksay, Simultaneous liquid viscosity and density determination with piezoelectric unimorph cantilevers, *J. Appl. Phys.*, 2001, **89**(2), 1497–1505.
- 48 J. Kim, J. Park, K. Na, S. Yang, J. Baek and E. Yoon, *et al.*, Quantitative evaluation of cardiomyocyte contractility in a 3D microenvironment, *J. Biomech.*, 2008, **41**, 2396–2401.
- 49 R. D. Kamm, R. M. Nerem and K. J. Hsia, Cells into systems, *Mech. Eng.*, Nov 2010, 30–34.
- 50 S. Chlopcikova, J. Psotova and P. Miketova, Neonatal rat cardiomyocytes—a model for the study of morphological, biochemical and electrophysiological characteristics of the heart, *Biomed. Pap.*, 2001, **145**(2), 49–55.
- 51 K. Baar, R. Birla, M. O. Boluyt, G. H. Borschel, E. M. Arruda and R. G. Dennis, Self-organization of rat cardiac cells into contractile 3-D cardiac tissue, *FASEB J.*, 2005, **19**, 275–277.
- 52 K. Shapira-Schweitzer, M. Habib, L. Gepstein and D. Seliktar, A photopolymerizable hydrogel for 3-D culture of human embryonic stem cell-derived cardiomyocytes and rat neonatal cardiac cells, *J. Mol. Cell. Cardiol.*, 2009, **46**, 213–224.
- 53 H. J. Berger, S. K. Prasad, A. J. Davidoff, D. Pimental, O. Ellingsen and J. D. Marsh, *et al.*, Continual electric field stimulation preserves contractile function of adult ventricular myocytes in primary culture, *Am. J. Physiol.*, 1994, **266**(1 Pt 2), H341–H349.
- 54 T. Bruegmann, D. Malan, M. Hesse, T. Beiert, C. J. Fuegemann and B. K. Fleischmann, *et al.*, Optogenetic control of heart muscle *in vitro* and *in vivo*, *Nat. Methods*, 2010, **7**(11), 897–900.
- 55 A. B. Arrenberg, D. Y. Stainier, H. Baier and J. Huisken, Optogenetic control of cardiac function, *Science*, 2010, **330**(6006), 971–974.